**Preprints of the 21st IFAC World Congress (Virtual)**
**Berlin, Germany, July 12-17, 2020**

# A control oriented pattern for plant design: the homogeneous population pattern

**R. Lucchese** * **K. Atta** * **M. Guay** **

* *Department of Computer Science, Electrical and Space engineering, Luleå University of Technology, Sweden*
*(e-mails:* ricluc|kahatt@ltu.se).
** *Department of Chemical Engineering, Queen's University, Canada*
*(e-mail:* guaym@queensu.se)

Abstract: We consider an adaptive control problem for a homogeneous population of systems that operate in close conditions. Drawing a connection to Design of Experiments (DoE), we study an extremum seeking controller that operates the population economically by either minimizing a group cost or maximizing a group utility. The controller is formalized in full detail within a dynamic setting that extends the previous treatment. The applicability and effectiveness of the strategy is commented upon and supported through different examples. We argue that this class of control systems should be addressed as a design pattern where possible in view of its capacity to enable both simple and effective online optimizing control strategies.

*Keywords:* Plant design patterns, Control oriented plant design, Homogeneous population of systems, Extremum seeking, Design of experiments

## 1. INTRODUCTION

The selection and tuning of opportune control structures are central to the design of effective process automation. In general, accomplishing the design task mandates a fair application of both art and formal methods to account for the specific requirements and performance/complexity/cost trade-offs (Seborg et al., 2010). To complicate matters, the control engineer is often not perceived as a principle stakeholder throughout the plant design process. This eventually opens to a disproportion between the effort required to design the control system and the benefit from attaining the performance.

Here, we propose a plant design pattern that enables an intuitive adaptive control strategy based on running parallel simultaneous experiments. More formally, we study homogeneous populations of systems that operate in close conditions and consider how to optimize a group cost or utility online. Homogeneous populations of this kind emerge naturally across different application scenarios: on one hand, scaling manufacturing processes necessitates the modularization of the product itself; on the other hand, meeting both capacity demands and redundancy guarantees leads to replicating the infrastructures at the final plant site. In solar power installations, for example, the replicated system can be identified with the single photovoltaic (PV) panel; moreover, nearby panels can be assumed to operate in close conditions, thus forming a homogeneous population (see Figure 1). Other application scenarios characterized by similar considerations include a range of energy intensive processes such as Heating, Ventilation, and Air-Conditioning (HVAC) systems, heat pump facilities servicing district heating loops, wind and hydroelectric turbine plants. In all these settings, the economic operation of the single unit requires tuning only a small number of manipulable variables (less than three or four). However, the optimal tuning depends strongly and nonlinearly on multiple time-varying boundary conditions. Moreover, the latter exogenous inputs and the overall nonlinear model of the objective might not be available online. With this context, here we argue that homogeneous populations of systems should be addressed not only on a case by case basis, when it is required to meet design requirements, but also as a plant design *pattern*, whenever the benefits of optimal operations may exceed the acquisition cost of deploying replicated infrastructures.

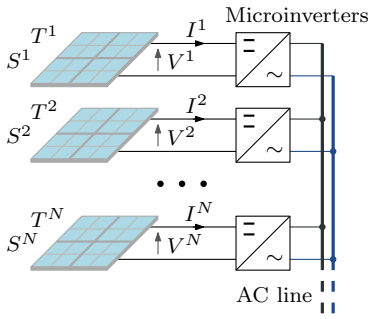


Figure 1. An array of PV panels is a fitting example of a homogeneous population of systems in which an adaptive controller optimizes the power production. We address this example in Section 8.

*Literature review.* Attaining the performance in economic control problems presents the challenge of tracking the optimal operating point online. When detailed plant knowledge is available, model-based controllers can form optimal decisions on the basis of state and output predictions (Ellis et al., 2016). However, developing the underlying model requires upfront effort and may result in numerically

challenging online optimal control problems. Alternative model-free strategies must retrieve some plant knowledge online in order to steer the process, typically by using variants of a perturb and observe scheme. For instance, the information generation process in Extremum Seeking Control (ESC) uses an additive dither that is applied to the control signal. The dither signal then disrupts the plant operations whenever a new optimization cycle is required and for the length of the optimization (Tan et al., 2008). Control strategies for replicated infrastructures have been analysed previously. However, the existing literature lacks to recognize the underlying plant design as a control oriented pattern, missing to highlight the relevance and potential of homogeneous populations in this context. Srinivasan (2007) considers a setup similar to ours, using finite differences to estimate the profitable direction, limiting to static convex objectives and to a population of perfectly identical control systems. Woodward et al. (2009) introduces plant dynamics but in the context of single-input systems and populations of size two, moreover neglecting any exogenous signals perturbing the group's operations.

*Statement of contributions.* We identify a plant design pattern that naturally emerges in settings where deploying replicas of the same infrastructure is necessary to attain the resource capacity. Although widespread, this pattern is neither recognized nor addressed systematically as such. We then study an intuitive adaptive control strategy that applies to generic populations of homogeneous systems. We show that as long as all instances in the population operate in close conditions, an experimental design may be exploited to extract online information on the profitable directions and eventually bring the operations near the optimal group cost or group utility. We frame formally the proposed adaptive control strategy and detail different in silico application scenarios to demonstrate its efficacy. Completing previous results, we consider 1) multivariable settings in which 2) the single instances forming the population need not be identical and 3) are allowed to have dynamics. Moreover, 4) we suggest to treat the online derivative reconstruction problem within a formal Design of Experiments (DoE) framework.

*Organization of this manuscript.* Section 2 details our framework. Section 3 formalizes the population based adaptive controller. Section 4 discusses the design of the simultaneous experiments. Section 5 highlights the convergence results. Section 6, 7, and 8 demonstrate the efficacy of the proposed controller over selected practically relevant scenarios. Finally, Section 9 collects concluding remarks and future directions.

## 2. BACKGROUND

We consider a population of $N \in \mathbb{N}_{>0}$ control systems in the following parametric family

$$\sigma(\boldsymbol{\theta}) \doteq \begin{cases} \dot{\boldsymbol{x}} = f(\boldsymbol{x}, \boldsymbol{u}, \boldsymbol{w}, \boldsymbol{\theta}) \\ y = h(\boldsymbol{x}, \boldsymbol{u}, \boldsymbol{w}, \boldsymbol{\theta}) \end{cases} \tag{1}$$

where $\boldsymbol{x} \in \mathcal{X} \subset \mathbb{R}^n$ is the state vector, $y \in \mathbb{R}$ is the scalar output, $\boldsymbol{u} \in \mathcal{U} \subset \mathbb{R}^m$ is the control value, $\boldsymbol{w} \in \mathcal{W} \subset \mathbb{R}^p$ captures the exogenous inputs, and $\boldsymbol{\theta} \in \Theta \subset \mathbb{R}^q$ are the parameters. The mappings $f, h$ are assumed sufficiently regular and the sets $\mathcal{X}, \mathcal{U}, \mathcal{W}, \Theta$ are compact. The population is described as a collection of noninteracting systems and denoted using

$$\Sigma \doteq \left(\sigma^1, \sigma^2, \cdots, \sigma^N\right), \tag{2}$$

where $\sigma^i \doteq \sigma(\boldsymbol{\theta}^i)$ for some fixed parameter $\boldsymbol{\theta}^i \in \Theta$. The state, manipulable, and exogenous variables of $\sigma^i$ are denoted with $\boldsymbol{x}^i$, $\boldsymbol{u}^i$, and $\boldsymbol{w}^i$, respectively: $\Sigma$ thus has $nN$ states and $(m+p)N$ inputs. The amount of variability induced by differing parameters $\boldsymbol{\theta}^i$ and exogenous inputs $\boldsymbol{w}^i$ is quantified through the following Lipschitz continuity assumption.

*Assumption 1.* (Population homogeneity). Let the indexes $i, j \in \{1, \dots, N\}$ denote a pair of two instances in $\Sigma$, let $\boldsymbol{x}_0^i, \boldsymbol{x}_0^j \in \mathcal{X}$ be their initial states at time $t = 0$, and denote their outputs by $y^i(t), y^j(t)$. Then, there exists constants $c_1, c_2, c_3, c_4, c_5 \in \mathbb{R}_{\geq 0}$, independent of $i$ and $j$, such that

$$\begin{aligned} \left\|y^i(t) - y^j(t)\right\|_\infty \leq c_1 e^{-c_2 t} \left\|\boldsymbol{x}_0^i - \boldsymbol{x}_0^j\right\|_\infty \\ + c_3 \left\|\boldsymbol{\theta}^i - \boldsymbol{\theta}^j\right\|_\infty + c_4 \sup_{0 \leq \tau \leq t} \left\|\boldsymbol{u}^i(\tau) - \boldsymbol{u}^j(\tau)\right\|_\infty \\ + c_5 \sup_{0 \leq \tau \leq t} \left\|\boldsymbol{w}^i(\tau) - \boldsymbol{w}^j(\tau)\right\|_\infty, \quad t \geq 0. \end{aligned} \tag{3}$$

Roughly speaking, the trajectories of any two instances $\sigma^i, \sigma^j$ resemble each other whenever the initial states, the inputs, and the parameters are sufficiently close.

We assume the following "driftless" behavior: applying constant inputs steers each instance in $\Sigma$ to a well defined steady state.

*Assumption 2.* (Driftless dynamics). There exist a mapping $\ell : \mathcal{U} \times \mathcal{W} \times \Theta \mapsto \mathcal{X}$ such that

$$f(\ell(\boldsymbol{u}, \boldsymbol{w}, \boldsymbol{\theta}), \boldsymbol{u}, \boldsymbol{w}, \boldsymbol{\theta}) = 0. \tag{4}$$

Under the standing assumptions, it is implied that also $\ell$ is Lipschitz continuous and has bounded gradient. The $N$ outputs $\{y^i\}$ of $\Sigma$ are understood as measurable operation costs or utilities to be optimized online. Without loss of generality, we define the steady state cost incurred by the $i$-th system in function of the manipulable and exogenous inputs as

$$J^i(\boldsymbol{u}^i, \boldsymbol{w}^i) \doteq h(\ell(\boldsymbol{u}^i, \boldsymbol{w}^i, \boldsymbol{\theta}^i), \boldsymbol{u}^i, \boldsymbol{w}^i, \boldsymbol{\theta}^i). \tag{5}$$

The following *group* cost is introduced to account for the operation of the entire population

$$J(\boldsymbol{u}^1, \dots, \boldsymbol{u}^N, \boldsymbol{w}^1, \dots, \boldsymbol{w}^N) \doteq \sum_{i=1}^{N} J^i(\boldsymbol{u}^i, \boldsymbol{w}^i). \tag{6}$$

For the sake of a compact notation, we will abuse $\{\boldsymbol{u}^i\}$ (and similarly $\{\boldsymbol{w}^i\}$) to denote also the $N$ ordered arguments $\boldsymbol{u}^1, \dots, \boldsymbol{u}^N$, and moreover write the group cost as $J(\{\boldsymbol{u}^i\}, \{\boldsymbol{w}^j\})$, or $J(\boldsymbol{u}, \{\boldsymbol{w}^j\})$ when implying $\boldsymbol{u}^i = \boldsymbol{u}$ for all $i = 1, \dots, N$.

*Remark 3.* We stress that not only the parameters affecting the individual instances $\sigma^i$ are unknown, also the underlying dynamics are unknown. This reflects a minimum information setting in which producing detailed a priori plant knowledge is impractical.

## 3. ADAPTIVE CONTROL VIA SIMULTANEOUS EXPERIMENTS

In the remainder, the control aim is to track the *unknown* optimal control value $\boldsymbol{u}^\star$ minimizing the group cost for $\Sigma$,

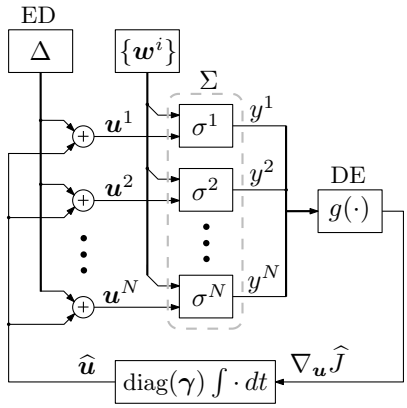


Figure 2. Block scheme for the adaptive control scheme exploiting $N$ simultaneous experiments over the homogeneous population $\Sigma$.

that is,

$$\boldsymbol{u}^\star \in \underset{\boldsymbol{u}\in\mathcal{U}}{\operatorname{argmin}}\ J(\boldsymbol{u}, \{\boldsymbol{w}^i\}). \tag{7}$$

A precondition required to motivate the problem setup and (7) is that each $\boldsymbol{w}^i$ either varies *slowly* in time or varies *little* in time (this is formalized later in Definitions 6 and 7). Since the parameters $\{\boldsymbol{\theta}^i\}$ and the exogenous inputs $\{\boldsymbol{w}^i\}$ cannot be supervised by the controller, the focus remains set on minimizing the section $\boldsymbol{u} \mapsto J(\boldsymbol{u}, \{\boldsymbol{w}^i\})$ and, thus, on learning the steepest descent direction $-\nabla_{\boldsymbol{u}} J$ online.

We propose to address the task at hand through the adaptive control strategy summarized graphically in Figure 2. The basic intuition is to run simultaneous experiments on the $N$ instances of $\Sigma$. In this scheme, the collection of outputs $\{y^i\}$ is aggregated to produce an estimate $\widehat{\nabla_{\boldsymbol{u}} J}$ of $\nabla_{\boldsymbol{u}} J$, which is then mapped to the current guess $\widehat{\boldsymbol{u}}$ of $\boldsymbol{u}^\star$. The closed loop dynamics, including the output feedback law, takes the state space form

$$\begin{cases} \dot{\boldsymbol{x}}^i = f(\boldsymbol{x}^i, \widehat{\boldsymbol{u}} + \boldsymbol{\delta}^i, \boldsymbol{w}^i, \boldsymbol{\theta}^i), \quad i = 1, \dots, N \\ y^i = h(\boldsymbol{x}^i, \widehat{\boldsymbol{u}} + \boldsymbol{\delta}^i, \boldsymbol{w}^i, \boldsymbol{\theta}^i), \quad i = 1, \dots, N \\ \dot{\widehat{\boldsymbol{u}}} = \operatorname{diag}(\boldsymbol{\gamma})\, g(y^1, \dots, y^N) \end{cases} \tag{8}$$

where $\boldsymbol{\delta}^i \in \mathbb{R}^m$, $i = 1, \dots, N$, are constant offsets injected into the $N$ systems, and $g : \mathbb{R}^N \to \mathbb{R}^m$ is a derivative estimator mapping the measured outputs into the gradient estimate $\widehat{\nabla_{\boldsymbol{u}} J}$. The vector of adaptation gains $\boldsymbol{\gamma} \in \mathbb{R}^m$ is entry-wise negative when $J$ represents a cost.

## 4. DESIGN OF THE SIMULTANEOUS EXPERIMENTS

An Experimental Design (ED) for the adaptive control scheme (8) is a set of offsets

$$\Delta \doteq \left\{\boldsymbol{\delta}^1, \boldsymbol{\delta}^2, \dots, \boldsymbol{\delta}^N\right\} \tag{9}$$

where the generic $\boldsymbol{\delta}^i$ is vector in $\mathbb{R}^m$. The ED is applied to the estimate $\widehat{\boldsymbol{u}}$ of the optimizer $\boldsymbol{u}^\star$ in (7) to produce $N$ measurable, simultaneous, experimental outcomes $\{y^i\}$. Observing the output trajectory of $\Sigma$ allows then the reconstruction of a response surface, conveying information on the local group cost gradient $\nabla_{\boldsymbol{u}} J$ and, by an opportune design, any higher order derivatives.

Broadly speaking, an effective Derivative Estimator (DE) $g$ can be designed by postulating either parametric or nonparametric models for the observations Brekelmans et al. (2005); Rasmussen and Williams (2010). Lacking global information, a numerically efficient local strategy is to project the observations onto a finite-dimensional linear functional space (for instance, a truncated Taylor expansion). This process yields a separable form

$$\begin{bmatrix} y^1 & y^2 & \dots & y^N \end{bmatrix}^\top = \begin{bmatrix} \mathbf{1} & \Phi \end{bmatrix} \begin{bmatrix} \alpha_0 \\ \boldsymbol{\alpha} \end{bmatrix} \tag{10}$$

where the matrix $\Phi \in \mathbb{R}^{N \times N'}$ is a function of $\{\boldsymbol{\delta}^i\}$, the multipliers $\alpha_0 \in \mathbb{R}$, $\boldsymbol{\alpha} \in \mathbb{R}^{N'}$ are estimands, and (10) may be understood as a regularized Least Squares (LS) problem. We observe moreover that lacking also a priori local knowledge of $J$'s features, $\boldsymbol{\alpha}$ must have dimension at least $m$ to allow the reconstruction of $\nabla_{\boldsymbol{u}} J$, inducing the following necessary condition [1]

$$N \geq N' + 1 \geq m + 1. \tag{11}$$

*Assumption 4.* (Population size). The size of the population $\Sigma$ satisfies (11).

Different strategies are considered in the literature under deterministic and noise stochastic settings. The $(\Delta, g)$ pair can be designed in terms of numerical approximations as, for instance, finite forward, backward, and central differences, or by using optimal DoE as discussed in Pronzato (2007); Brekelmans et al. (2005).

*Example 5.* When the focus is on minimizing the population size, that is $N = m+1$, one may consider the following Plackett-Burman ED

$$\begin{bmatrix} \mathbf{1} & \Phi \end{bmatrix} = H_N D, \tag{12}$$

where $H_N \in \{-1, 1\}^{N \times N}$ is Hadamard and $D = \operatorname{diag}(1, d_1, d_2, \dots, d_m) \succ \mathbf{0}$ is a positive matrix collecting the offsets' amplitudes. Notice that (12) implies an affine local surrogate model. The parameters of $D$ must be tuned by the designer, adapting the ED to the range of the actuators so as to achieve a faithful reconstruction of the response surface. With this choice, the ED in (8) and (9) is embedded within the rows of the regressor,

$$\boldsymbol{\delta}^i_h = (H_N D)_{i,h+1} \quad 1 \leq h \leq m,\ 1 \leq i \leq N \tag{13}$$

and, since $H_N H_N^\top = N\boldsymbol{I}$, one has the following LS estimator of the gradient

$$g(y^1, \dots, y^N) \doteq \begin{bmatrix} \mathbf{0} & \boldsymbol{I}_m \end{bmatrix} D^{-1} \frac{H_N^\top}{N} \begin{bmatrix} y^1 & \cdots & y^N \end{bmatrix}^\top. \tag{14}$$

We refer to Brekelmans et al. (2005) for the details on the optimality properties of Plackett-Burman designs.

ED-DE pairs such as (13)-(14) produce an exact guess of $\nabla_{\boldsymbol{u}} J$ for the special case of a population of static, linear, and identical instances. More generally, it becomes necessary to consider an operational envelop in order to quantify the effects of the nonlinearities and the different dynamical behaviors induced by $\{\boldsymbol{\theta}^i\}$ and $\{\boldsymbol{w}^i\}$. Define the radius of a set $E$ as

$$\rho(E) \doteq \sup_{\boldsymbol{e}_1, \boldsymbol{e}_2 \in E} \|\boldsymbol{e}_1 - \boldsymbol{e}_2\|_\infty. \tag{15}$$

*Definition 6.* (Static envelope). The static envelope $\mathcal{E}_s$ with radii $r_{\boldsymbol{w}}, r_{\boldsymbol{\theta}}$ is the set

[1] The validity of (11) extends then to settings where estimating the higher derivatives is of interest, and in which $N'$ must be larger than the number of partial derivatives to be inferred.

$$\mathcal{E}_s(r_{\boldsymbol{w}}, r_{\boldsymbol{\theta}}) \doteq \big\{ \boldsymbol{w}^1, \dots, \boldsymbol{w}^N, \boldsymbol{\theta}^1, \dots, \boldsymbol{\theta}^N \in \mathcal{W}^N \times \Theta^N \text{ s.t. } \rho(\{\boldsymbol{w}^i\}) < r_{\boldsymbol{w}}, \rho(\{\boldsymbol{\theta}^i\}) < r_{\boldsymbol{\theta}} \big\}. \tag{16}$$

*Definition 7.* (Dynamic envelope). We say that $\Sigma$ operates within the dynamic envelop with positive radii $(r_{\boldsymbol{x}}, r_{\boldsymbol{u}}, r_{\boldsymbol{w}}, r_{\boldsymbol{\theta}}, r_{\dot{\boldsymbol{w}}}, r_{\dot{\boldsymbol{u}}})$ if for all positive times $t \geq 0$ there holds $\{\boldsymbol{w}^i\}, \{\boldsymbol{\theta}^i\} \in \mathcal{E}_s(r_{\boldsymbol{w}}, r_{\boldsymbol{\theta}})$ together with

$$\rho(\{\boldsymbol{x}_0^i - \ell(\boldsymbol{u}^i, \boldsymbol{w}^i, \boldsymbol{\theta}^i)\}) < r_{\boldsymbol{x}}, \quad \sup_{t\geq 0} \rho(\{\boldsymbol{u}^i(t)\}) < r_{\boldsymbol{u}}, \quad \sup_{t\geq 0} \rho(\{\dot{\boldsymbol{w}}^i(t)\} \cup \{0\}) < r_{\dot{\boldsymbol{w}}}, \quad \sup_{t\geq 0} \rho(\{\dot{\boldsymbol{u}}^i(t)\} \cup \{0\}) < r_{\dot{\boldsymbol{u}}}, \tag{17}$$

The set of tuples of $N$ initial states, $2N$ input signals, and $N$ parameters simultaneously satisfying these conditions is denoted by $\mathcal{E}_d(r_{\boldsymbol{x}}, r_{\boldsymbol{u}}, r_{\boldsymbol{w}}, r_{\boldsymbol{\theta}}, r_{\dot{\boldsymbol{w}}}, r_{\dot{\boldsymbol{u}}})$.

The characterization in (1) guarantees that arbitrarily accurate estimators $g$ may be designed as long as the $N$ instances of $\Sigma$ operate in sufficiently close conditions and the second order derivatives of $\nabla_{\boldsymbol{uu}} J$ are uniformly bounded.

*Definition 8.* We say that the pair $(\Delta, g)$ incurs a steady state estimation error at most $\varepsilon > 0$ over the envelope $\mathcal{E}_s(r_{\boldsymbol{w}}, r_{\boldsymbol{\theta}})$ if

$$\sup_{\substack{\boldsymbol{u}\,:\,\boldsymbol{u}+\boldsymbol{\delta}^i \in \mathcal{U},\, 1\leq i\leq N \\ \{\boldsymbol{w}^i\}, \{\boldsymbol{\theta}^i\} \in \mathcal{E}_s(r_{\boldsymbol{w}}, r_{\boldsymbol{\theta}})}} \left\| e(\boldsymbol{u}, \{\boldsymbol{w}^i\}) \right\|_\infty < \varepsilon, \tag{18}$$

with

$$e \doteq \nabla_{\boldsymbol{u}} J(\boldsymbol{u}, \{\boldsymbol{w}^i\}) - g\left(J^1(\boldsymbol{u}+\boldsymbol{\delta}^1, \boldsymbol{w}^1), \dots, J^N(\boldsymbol{u}+\boldsymbol{\delta}^N, \boldsymbol{w}^N)\right).$$

*Proposition 9.* Assume $\nabla_{\boldsymbol{uu}} J$ uniformly bounded. Then, for any pair $(\Delta, g)$ as in (13)-(14) and $\varepsilon > 0$ there exists a non-empty envelop $(r_{\boldsymbol{w}}, r_{\boldsymbol{\theta}})$ and a radius $r_{\boldsymbol{\delta}} > 0$ such that the new ED-DE pair

$$\left(s\Delta, s^{-1} g\right) \tag{19}$$

with constant $s \doteq r_{\boldsymbol{\delta}}/\rho(\Delta)$, incurs a static error at most $\varepsilon$.

The proof of this statement, here omitted in the interest of space, follows from the fact that Assumption 1 renders Lipschitz continuous steady state costs (5).

In practice, tuning of the ED, and in particular its radius $\rho(\Delta)$, may be performed on the basis of either a priori experimental knowledge or using lack-of-fit indicators for (10). We notice then that the attainable accuracy will be naturally limited by the presence of process and measurement noise which can nevertheless be formally captured by the near-optimality guarantees established in the following section.

## 5. CLOSED-LOOP NEAR OPTIMALITY

The following open-loop result formalizes the intuition that as long as the population operates in close conditions, and the rate of change of the common control signal (denoted with $\widehat{\boldsymbol{u}}$ in (8)) is sufficiently small, then the simultaneous experiments setup of the previous section is able to produce an online gradient estimate suitable to drive the ESC.

*Proposition 10.* If the pair $(\Delta, g)$ in Proposition 9 is $\varepsilon_1$-accurate over the envelope $\mathcal{E}_s(r_{\boldsymbol{w}}, r_{\boldsymbol{\theta}})$ then there exist radii $r_{\boldsymbol{x}}, r_{\boldsymbol{u}}, r_{\dot{\boldsymbol{w}}}, r_{\dot{\boldsymbol{u}}} \in \mathbb{R}_{>0}$ such that

$$\left\| \nabla_{\boldsymbol{u}} J\left(\boldsymbol{u}(t), \{\boldsymbol{w}^i(t)\}\right) - g\left(y^1(t), \dots, y^N(t)\right) \right\|_\infty < 2\varepsilon_1,$$

uniformly in $t \geq 0$, whenever $\Sigma$ operates in the dynamic envelop $\mathcal{E}_d(r_{\boldsymbol{x}}, r_{\boldsymbol{u}}, r_{\boldsymbol{w}}, r_{\boldsymbol{\theta}}, r_{\dot{\boldsymbol{w}}}, r_{\dot{\boldsymbol{u}}})$.

**Proof.** A sketch of the proof is as follows. For the statement to hold it is sufficient to show that for any positive constant $c \in \mathbb{R}_{>0}$ there exist small radii $r_{\boldsymbol{x}}, r_{\boldsymbol{u}}, r_{\dot{\boldsymbol{w}}}, r_{\dot{\boldsymbol{u}}} \in \mathbb{R}_{>0}$ such that the output trajectories of $\Sigma$ satisfy

$$\left\| y^i(t) - J^i\left(\boldsymbol{u}(t) + \boldsymbol{\delta}^i, \boldsymbol{w}^i(t)\right) \right\|_\infty < c \quad \forall\, 1 \leq i \leq N, t \geq 0. \tag{20}$$

Notice that (20) can be interpreted as a quasi steady state operating condition. For slowly varying systems of this kind, bounds on the dynamic envelope radii can be recovered explicitly as in (Khalil, 2002, Theorem 9.3) under the provision that an opportune control Lyapunov function $V(\boldsymbol{z}^i, \boldsymbol{u}^i, \boldsymbol{w}^i, \theta^i)$ exists for the family of shifted dynamics

$$\dot{\boldsymbol{z}}^i = f(\boldsymbol{z}^i + h(\boldsymbol{u}^i, \boldsymbol{w}^i, \theta^i), \boldsymbol{u}^i, \boldsymbol{w}^i, \boldsymbol{\theta}^i), \tag{21}$$

with $\boldsymbol{z}^i \doteq \boldsymbol{x}^i - h(\boldsymbol{u}^i, \boldsymbol{w}^i, \theta^i)$, $\boldsymbol{u}^i, \boldsymbol{w}^i, \boldsymbol{\theta}^i \in \mathcal{U} \times \mathcal{W} \times \Theta$. Such $V$ exists by the assumptions of Section 2 and the converse Lyapunov result of Lemma 9.8 in Khalil (2002). An estimate for the required $c$ can then be drawn from knowledge of $\|g\|$. ■

*Definition 11.* (Near optimality). Given $\varepsilon_2 > 0$, we say that the adaptive controller (8) is $\varepsilon_2$ nearly optimal for the dynamic operation envelope $\mathcal{E}_d(r_{\boldsymbol{x}}, r_{\boldsymbol{u}}, r_{\boldsymbol{w}}, r_{\boldsymbol{\theta}}, r_{\dot{\boldsymbol{w}}}, r_{\dot{\boldsymbol{u}}})$ if

$$\limsup_{t\to+\infty} \left| J\left(\widehat{\boldsymbol{u}}(t), \{\boldsymbol{w}^i(t)\}\right) - J(\boldsymbol{u}^\star(t), \{\boldsymbol{w}^i(t)\}) \right| < \varepsilon_2. \tag{22}$$

We then have the following closed-loop asymptotic practical stability result.

*Theorem 1.* Assume the optimizer $u^\star$ in (7) to be univocally identified for each operating condition. Then, for every given $\varepsilon_2 > 0$, there exists *i*) an ED-DE pair in Proposition 10, *ii*) an open-loop dynamic operating envelope $\mathcal{E}_d$, and *iii*) an adaptation gain $\boldsymbol{\gamma} \in \mathbb{R}^m_{<0}$ such that the closed-loop dynamics (8) let $\Sigma$ operate within $\mathcal{E}_d$ and moreover the output feedback guarantees the $\varepsilon_2$ near-optimality condition in (22).

**Proof.** A sketch of the proof proceeds as follows. Proposition 9 suggests an ED-DE pair with tunable steady state accuracy. Proposition 10 asserts that the gradient estimation error during transients can be uniformly bounded as long as the system is slowly varying. This latter condition is attained by choosing a vector of adaptation gains with $\|\boldsymbol{\gamma}\|$ sufficiently small. Tuning of the ED-DE pair instead guarantees an arbitrarily accurate reconstruction of $\nabla_{\boldsymbol{u}} J$ which in turn allows the system to be steered within the $\epsilon_2$ nearly optimal neighborhood of $\boldsymbol{u}^\star$ . ■

*Remark 12.* We stress that the controller poses no additional assumptions on generally challenging features of the dynamics such as, for example, non-minimum phase behaviors. In fact, more generally, the $N$ instances in $\Sigma$ may be characterized by drastically different state dynamics as long as the same steady state behavior is approximately retained.

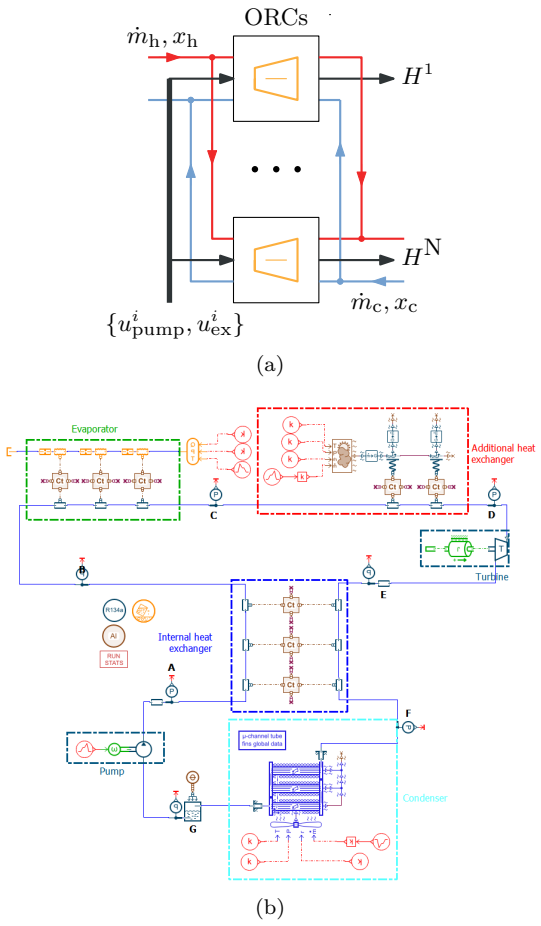


Figure 3. In (a), an array of Organic Rankine Cycles (ORCs) uses a common heat source and a common heat sink to produce the output work $\{H^i\}$. The overall effectiveness is affected by the rotational speeds of the pump and expander ($u^i_\mathrm{pump}$ and $u^i_\mathrm{ex}$, respectively) in each unit. In (b), implementation of the ORC instances in Siemens's Amesim.

## 6. EXAMPLE: ORC-BASED GENERATORS

ORCs are increasingly finding application in contexts where generating electricity from low grade waste heat provides operational benefits. Exemplative scenarios range from geothermal plants to large cruise ships. We refer to Quoilin et al. (2013) for a survey of economic and technological aspects of ORCs.

Consider the plant schematized in Figure 3 in which a population of ORCs operates with the same hot side (heat source) and cold side (heat sink) mass flow $(\dot{m}_\mathrm{h}, \dot{m}_\mathrm{c})$ and temperature conditions $(x_\mathrm{h}, x_\mathrm{c})$. The generic $i$-th ORC unit has two manipulable controls $u_\mathrm{pump}$ and $u_\mathrm{ex}$ corresponding, respectively, to the Revolutions per Minute (RPM) of the cycle's pump and expander parts. The operation objective is to maximize the utility

$$J(u_\mathrm{pump}, u_\mathrm{ex}, \{\dot{m}^i_\mathrm{h}, x^i_\mathrm{h}, \dot{m}^i_\mathrm{c}, x^i_\mathrm{c}\}) \doteq \sum_{i=1}^{N} H^i(u_\mathrm{pump} + \delta^i_\mathrm{pump}, u_\mathrm{ex} + \delta^i_\mathrm{ex}), \tag{23}$$

where $H^i$ is the output work produced by the $i$-th ORC system in function of the controls, and we set $\dot{m}^i_\mathrm{h} = \dot{m}_\mathrm{h}/N, \dot{m}^i_\mathrm{c} = \dot{m}_\mathrm{c}/N, x^i_\mathrm{h} = x_\mathrm{h}, x^i_\mathrm{c} = x_\mathrm{c}$. The ED is designed as in Example 5 with $D = \mathrm{diag}\,(1, 20, 2)$ and considering the adaptation gain $\boldsymbol{\gamma} = [2000\ 1]^\top$. The high gain $\boldsymbol{\gamma}_1$ is chosen to pair with the week sensitivity of (23) with respect to the pump velocity $u_\mathrm{pump}$. A conservative tuning is chosen to prevent sudden changes in the liquid-vapor mixture properties at the condensers and evaporators.

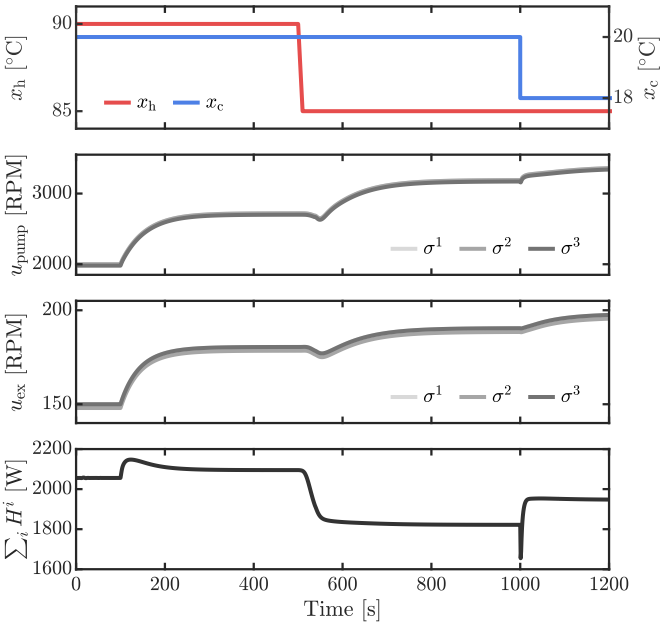


Figure 4. A control-oriented design of the ORC plant enables a simple and intuitive adaptive control strategy that tracks the maximum output work defined in (23) in spite of varying operating conditions, plant nonlinearities, and lack of detailed plant knowledge.

We evaluate the proposed adaptive scheme within the following scenario. The evaporators on the hot side are each supplied with hot water with constant volumetric flow rate of 0.79 l/s, while the condensers on the cold side are cooled using moist air with 40 % relative humidity and constant rate of 0.33 kg/s. Steps in the inflow temperatures $x_\mathrm{c}, x_\mathrm{h}$ are introduced at times $t = 500$ s and $t = 1000$ s, see Figure 4. We start the controller's state with the suboptimal guesses $u_\mathrm{pump} = 2000$ RPM and $u_\mathrm{ex} = 150$ RPM and let it supervise the array from time $t = 100$ s onward. The controller first drives the system toward the optimal operating conditions recovering from the suboptimal initial settings, and then continues to track the maximum utility despite changes in the exogenous inputs and the induced transients.

## 7. EXAMPLE: A HEAT RECOVERY NETWORK

A heat recovery plant using an array of Heat Exchangers (HXs) is shown in Figure 5. In the proposed scenario, the heat removed from a production site is injected into a consumer-side loop without allowing the mixing of the production-side and consumer-side coolants. To attain the heat transfer capacity an array of heat exchangers is deployed, each endowed with independent flow actuators on both the hot and cold sides of the unit. These manipulable flow rates are denoted using $\dot{m}^i_\mathrm{h}$ and $\dot{m}^i_\mathrm{c}$. The exogenous inputs to each instance are the supply temperature of the

coolant on the hot-side, $x^i_{\mathrm{h,i}}$ and the return temperature $x^i_{\mathrm{c,i}}$ at the cold-side inlet ports of the HX units. We assume that water is used as the coolant medium, and each flow actuator is modeled as a first-order system incurring an economic operation cost $\dot{v} \mapsto P(\dot{v})$ cubic in the volumetric rate that is produced. The rate of heat transfer from the production to the consumer loop at each HX is denoted with $q^i$.

The control objective is to track the unknown rate of heat consumption $Q_c(t)$ while minimizing the total power consumption at the pump actuators. Within the scope of this manuscript we capture the control task through

$$J(\{\dot{v}_{\mathrm{h,i}}, \dot{v}_{\mathrm{c,i}}\}, \{Q_{\mathrm{c}}\}) \doteq N \cdot P(\dot{v}_{\mathrm{h,i}}) + N \cdot P(\dot{v}_{\mathrm{c,i}}) + \lambda\Big(Q_{\mathrm{c}} - \sum_{i=1}^{N} q^i\Big)^2, \tag{24}$$

and therefore take into account the soft-constraint induced by the heat transfer matching condition using a barrier term with penalty multiplier $\lambda \in \mathbb{R}_{>0}$.

The volumetric rates on each side of the HX units are assimilated to the controls. The corresponding mass rates $\{\dot{m}^i_{\mathrm{h}}, \dot{m}^i_{\mathrm{c}}\}$ are evaluated given the density of water at the temperature of the corresponding flow. We adopt a static $\epsilon$-Number of Transfer Units (NTU) model to capture the heat transfer rates $\{q^i\}$. In particular, given the mass flow rates and the inflow temperature on both sides of each HX we consider a counterflow setup for which Bergman et al. (2011)

$$\begin{aligned} &C_{\mathrm{c}} = \dot{m}_{\mathrm{c}} c_{\mathrm{p}}(x_{\mathrm{c,i}}), \quad C_{\mathrm{h}} = \dot{m}_{\mathrm{h}} c_{\mathrm{p}}(x_{\mathrm{h,i}}), \\ &\underline{C} = \min\{C_{\mathrm{c}}, C_{\mathrm{h}}\}, \quad \overline{C} = \max\{C_{\mathrm{c}}, C_{\mathrm{h}}\}, \\ &C_{\mathrm{r}} = \underline{C}/\overline{C}, \quad \overline{Q} = \underline{C}(x_{\mathrm{h,i}} - x_{\mathrm{c,i}}), \\ &\epsilon = \frac{1 - \exp\left(-\mathrm{NTU}(1 - C_{\mathrm{r}})\right)}{1 - C_{\mathrm{r}} \exp\left(-\mathrm{NTU}(1 - C_{\mathrm{r}})\right)}, \quad q = \epsilon \overline{Q}, \end{aligned} \tag{25}$$

where $x \mapsto c_{\mathrm{p}}(x)$ denotes the specific heat of water at temperature $x$. The vector $\boldsymbol{\theta} = [\tau \ \mathrm{NTU}]^\top$ subsumes then the parameters of each instance in $\Sigma$, namely the time constant of the pump actuators and the number of transfer units characterizing the HXs.

The heat recovery performance when the plant is supervised by the proposed adaptive controller is evaluated in Figure 6 under varying heat production and consumption rates $Q_{\mathrm{p}}, Q_{\mathrm{c}}$. We used $\tau = 60$, $\mathrm{NTU} = 3$, $D = \mathrm{diag}\,(1, 0.01, 0.01)$ and $\boldsymbol{\gamma} = 0.001 \cdot [1 \ 1]^\top$. The controller prefers to decrease the flow rate on the consumer side when there is a thermal energy surplus on the production side. This results in accurately matching the consumers' demand. However, as the consumption exceeds the production, the flow rate $\dot{v}_{\mathrm{c}}$ increases to accommodate the demand. Toward the end of the simulation period, the heat resources within the production loop deplete, sinking the water temperatures, and impairing the operation of the controller which becomes unable to track the requested transfer rates.

## 8. EXAMPLE: PV PANELS ARRAY

As a further exemplative scenario we consider a Maximum power point tracking (MPPT) application for PV panels (see Figure 1). To simplify the discussion, taking into account space constraints, we consider a population of two panels connected in parallel. For the numerical analysis, we adopt the following static $I$-$V$ characteristic

$$I = i_s(T,S) - i_0(T)\left[\exp\left(\frac{\frac{V}{n_s} + IR_s}{NV_t(T)}\right) - 1\right] - \left(\frac{\frac{V}{n_s} + IR_s}{R_p}\right)$$

where $V$ and $I = I(V,T,S)$ are the voltage and current output of the panel, $T$ is the operating temperature, $S$ is the power irradiated on the cells, and moreover

$$\begin{aligned} i_s(T,S) &= (I_s + k_i(T - T_r))\,\frac{S}{10^3}, \quad V_t(T) = \frac{kT}{q}, \\ i_0(T) &= I_0\left(\frac{T}{T_r}\right)^3 \exp\left[\frac{E_g}{NV_t(T)}\left(\frac{T}{T_r} - 1\right)\right], \end{aligned} \tag{26}$$

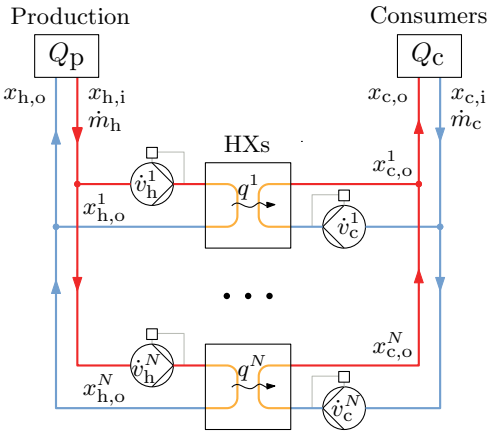


Figure 5. A heat exchanger network with three exchange elements requires supervision of the mass rates on the production and consumer sides to optimize (24).

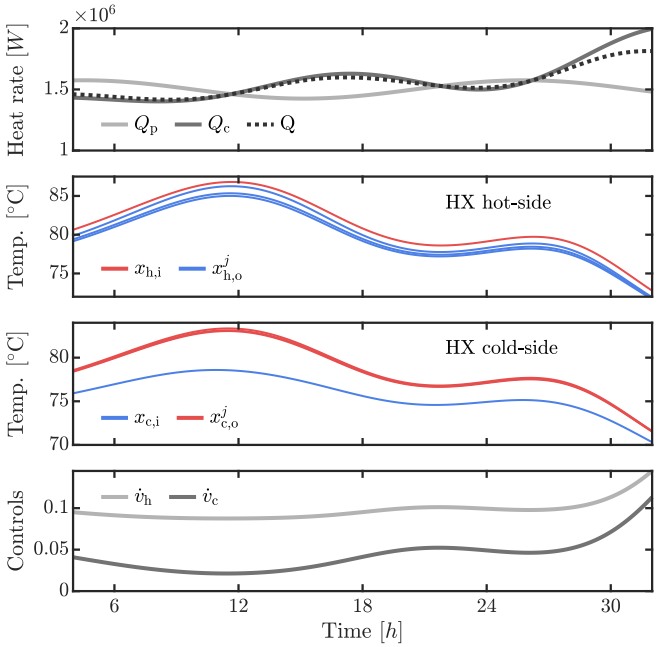


Figure 6. Heat recovery performance of the proposed adaptive controller applied to the example of Figure 5. Varying supply and consumption rates are designed in the top panel. The inflow and outflow water temperatures at the HXs units are shown in the second and third panels. The bottom panels depicts the controls.

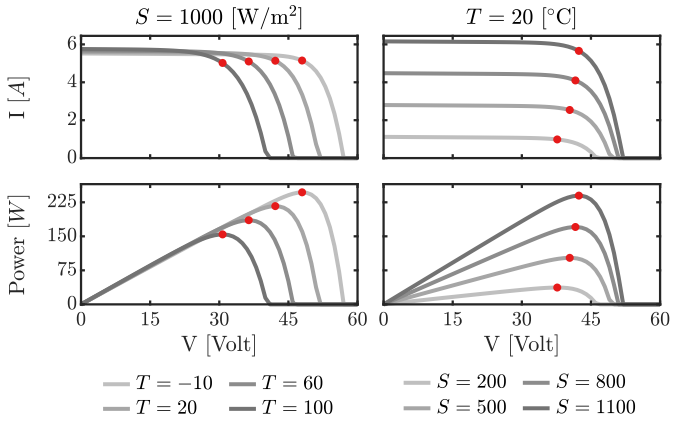


Figure 7. $I$-$V$ and power characteristics of the PV panel model considered in Section 8 for different values of the operating temperature $T$ and irradiation $S$. The maximum power points are highlighted in red.

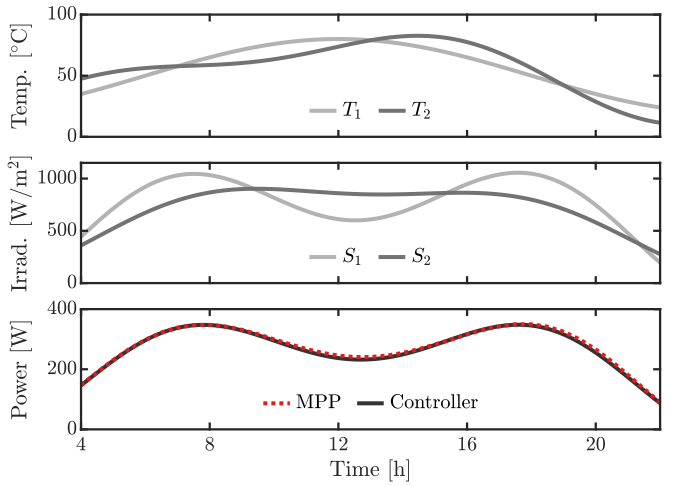


Figure 8. Example of Section 8: Performance of the adaptive controller compared to the optimal MPPT solution.

with $q$ denoting the elementary charge, $k$ the Boltzmann's constant, and $\boldsymbol{\theta} = [n_s\ R_s\ N\ R_p\ I_s\ k_i\ T_r\ E_g]^\top$ characteristic parameters of the panel (see Luque and Hegedus (2003) for details). The parameters are chosen as in Ghaffari et al. (2014) and reflect the properties of a Sanyo 215N device. The characteristic $I$-$V$ and power profiles are shown in Figure 7.

In this setup, the voltage $V$ can be assimilated to the control variable, while the temperature and irradiation are exogenous inputs. The control aim is then to operate the panels to maximize the total power production

$$J\left(V, \{T^i, S^i\}\right) = \sum_{i=1}^{2} V \cdot I^i(V, T^i, S^i). \tag{27}$$

To assess the proposed control scheme we consider the ED (13) with $D = \mathrm{diag}\,(1, 0.5, 0.5)$ and set $\gamma = 0.005$. The performance of the adaptive control scheme are compared to the optimal MPPT solution under varying irradiance and temperature conditions in Figure 8. The bottom panel, in particular, shows how the proposed controller is able to accurately track the theoretical MPP evaluated assuming exact knowledge of the exogenous inputs.

## 9. CONCLUSIONS

We argue that homogeneous populations of systems should be addressed as a control oriented design pattern rather then merely a necessity when multiple modular systems need to be deployed to meet the operation requirements. To support this argument we detail and evaluate an ESC strategy that exploits simultaneous experiments to infer the local gradient of the group cost or group utility. Several exemplative scenarios are considered in which a homogeneous population plant design becomes relevant in order to attain the required capacity and redundancy. It is of interest to note that plant configurations such as those in Figures 3 and 5 are natural in the sense that they can realize the optimal performance by operating with the highest temperature gap between the hot and cold side inflows.

Upcoming work focuses the detailed treatment of the formal results, including settings with process and measurement noise, and output constrained control problems. Of practical relevance is the application of these strategies to the online optimization of HVAC systems.

## REFERENCES

Bergman, T.L., Lavine, A.S., Incropera, F.P., and DeWitt, D.P. (2011). *Fundamentals of Heat and Mass Transfer*.

Brekelmans, R.C.M., Driessen, L.T., Hamers, H.J.M., and den Hertog, D. (2005). Gradient estimation schemes for noisy functions. *Journal of Optimization Theory and Applications*.

Ellis, M., Liu, J., and Christofides, P.D. (2016). *Economic Model Predictive Control: Theory, Formulations and Chemical Process Applications*. Springer.

Ghaffari, A., Krstić, M., and Seshagiri, S. (2014). Power optimization for photovoltaic microconverters using multivariable newton-based extremum seeking. *IEEE Transactions on Control Systems Technology*.

Khalil, H.K. (2002). *Nonlinear Systems*. Prentice Hall.

Luque, A. and Hegedus, S. (2003). *Handbook of Photovoltaic Science and Engineering*. Wiley.

Pronzato, L. (2007). Optimal experimental design and some related control problems. *Automatica*.

Quoilin, S., Broek, M.V.D., Declaye, S., Dewallef, P., and Lemort, V. (2013). Techno-economic survey of organic rankine cycle (ORC) systems. *Renewable and Sustainable Energy Reviews*.

Rasmussen, C.E. and Williams, C.K.I. (2010). *Gaussian processes for machine learning*. MIT press.

Seborg, D.E., Mellichamp, D.A., Edgar, T.F., and Doyle III, F.J. (2010). *Process Dynamics and Control*. John Wiley & Sons.

Srinivasan, B. (2007). Real-time optimization of dynamic systems using multiple units. *International Journal of Robust and Nonlinear Control*.

Tan, Y., Nešić, D., and Mareels, I. (2008). On the choice of dither in extremum seeking systems: A case study. *Automatica*.

Woodward, L., Perrier, M., and Srinivasan, B. (2009). Improved performance in the multi-unit optimization method with non-identical units. *Journal of Process Control*.